



Integrated Coherent Transmit-Receive Optical Sub-Assembly (IC-TROSA) for Data Center Interconnects

Kazuya Nagashima^{*1, 2}, Yozo Ishikawa^{*1, 2}, Atsushi Izawa^{*1, 2}, Masayoshi Nishita^{*3},
Noritaka Matsubara^{*2}, Hiroyuki Ishii^{*2}, Thanakit Saeyang^{*4}, Masaki Kotoku^{*1, 2}

ABSTRACT There is a strong demand for highly integrated optical modules that can be incorporated into a small coherent optical transceiver to provide a high data rate density in next-generation metro area networks and data center interconnects. This paper presents a tiny Integrated Coherent Transmit-Receive Optical Sub-Assembly (IC-TROSA) that integrates a wavelength-tunable laser, an indium phosphide (InP)-based transmitter, and a planar lightwave circuit (PLC)-based receiver. Electrical-to-optical (E/O) and optical-to-electrical (O/E) bandwidths measure > 40 GHz, which is wide enough to support ≥ 400 Gb/s operations.

1. INTRODUCTION

With the spreading usage of a high-quality video streaming, social media and Smartphone, Internet Traffic has been rapidly increasing. A digital coherent optical transmission technology that combines a high performance digital signal processor (DSP) and a coherent detection has been developed to meet the growing demand for high transmission-capacity communication systems. The digital coherent optical communication systems with a transmission capacity of 100 Gb/s/ λ have been introduced into backbone long-distance optical networks using a wavelength-tunable laser for wavelength division multiplexing (WDM).

Recently, the digital coherent technology has also been applied to shorter-reach applications, such as metro-area networks and data center interconnects (DCI). In such applications, smaller optical transceivers that can be operated at higher speed are required to provide a high data-rate density. Consequently, the Optical Internetworking Forum (OIF), an industry standardization organization, has issued an implementation agreement (IA) for 400ZR¹, which states a target performance for the optical link with 400 Gb/s. The IA is meant to be applied to small optical transceivers such as Quad Small Form-factor Pluggable Double Density (QSFP-DD)². Furthermore, the 800-Gb/s optical link³, which requires twice the transmission speed, is also under discussion for future's optical

links. This organization also issued an IA for an Integrated Coherent Transmit-Receive Optical Sub-Assembly (IC-TROSA) as a compact optical module to realize such a small optical transceiver⁴. The IA specifies two types, Type-1 and Type-2, of highly integrated optical modules. The IC-TROSA Type-1 integrates a dual-polarization coherent modulator and a receiver in a single ball grid array (BGA)-type package, whose size is 22.5 (L) \times 15 (W) \times 3.6 (H) mm. The Type-1 is supposed to be integrated into an optical transceiver in combination with an external wavelength-tunable laser. On the other hand, the IC-TROSA Type-2 needs to include a wavelength-tunable laser in addition to these optical devices in a small gold box package of 30.0 (L) \times 15.1 (W) \times 6.5 (H) mm. Previously, we reported an ultra-compact low-power Nano-Integrable Tunable Laser Assembly (Nano-ITLA) using a distributed Bragg reflector/ring resonator monolithically integrated laser chip and an ultra-high-delta PLC-based wavelength locker. It has a size small enough that can be mounted in the QSFP-DD together with an IC-TROSA Type-1 and it exhibits good transmission characteristics at a 400-Gb/s optical link⁵. To further minimize the optical module footprint and reduce the number of components, the IC-TROSA Type-2 is an attractive optical module. We successfully designed and fabricated an IC-TROSA Type-2 for 400-Gb/s operation, which integrates the small ITLA, an InP-based transmitter and a PLC-based receiver in a single package. In this paper, we describe the design and characteristics of the IC-TROSA Type-2. Furthermore, we also report the development status for ≥ 800 -Gb/s operations that is required in future optical links.

^{*1} Next Generation Photonics Business Innovation Project Team

^{*2} R&D Division, Telecommunications & Energy Laboratories

^{*3} Fitel Product Division

^{*4} Furukawa FITEL (Thailand)

2. DESIGN

Figure 1 shows a schematic illustration of the top view of IC-TROSA Type-2. In our approach, we integrated a wavelength-tunable laser, consisting of a monolithic-integrated laser and a PLC-based wavelength locker, a transmitter with an InP-based modulator, and a receiver with a PLC-based coherent mixer in a hybrid manner to realize high performance while keeping a simple fabrication process. The wavelength-tunable laser and the modulator are located on separated thermo electric coolers (TECs) to control their temperatures individually. The optical module has receptacle-type LC connectors to attach optical fiber cables easily. A quad modulator driver (DRV) and a trans-impedance amplifier (TIA) transmit high-speed signals through a flexible printed circuit (FPC) board attached to the optical module. In order to achieve a low-cost optical system, a simple 2-lens system with a collimator lens and a focusing lens is implemented. The output light from the wavelength-tunable laser chip is collimated and divided, and then focused to be coupled into each of the devices. The branching ratio is 75% to the modulator, 22.5% to the coherent mixer and 2.5% to the wavelength locker, respectively.

Figure 2 shows a schematic illustration of the wavelength-tunable laser chip. The laser chip has 2 types of wavelength-selecting reflectors and a gain section. An

SOA is integrated at the output port to boost and control the output power. Local micro heating elements are formed on each reflector to enable the lasing wavelength to be tuned arbitrarily. The laser chip size is 3 (L) × 0.35 (W) mm. A schematic illustration of the PLC-based wavelength locker is shown in Figure 3. This PLC consists of a SiO₂-ZrO₂ core that has a high refractive index difference (Δ) of about 5%⁵, therefore the minimum bending radius of the waveguides can be small, and we achieved the miniaturized wavelength locker size of 1.7 (L) × 2.5 (W) mm. The wavelength-tunable laser module, which was previously developed and reported, achieved ±0.5 GHz of a wavelength locking accuracy over the operating case temperature range, and < 100 kHz of a narrow linewidth over the full C-band wavelength range⁶.

For the transmitter, we implemented an InP-based optical polarization division multiplexing IQ Mach-Zehnder (MZ) modulator and a 4-channel modulator DRV. The InP-based modulator has characteristics such as a lower insertion loss, lower half-wave modulation voltage (V_{π}) higher speed operation compared to those of silicon photonics (SiPh)-based modulators⁷. Figure 4 is a schematic illustration of the InP-based modulator. The optical input/output ports are deployed on the same facet in order to make a small footprint of the optical module. Spot size converters (SSC) are integrated in those ports to achieve a good coupling efficiency and to broaden the allowable

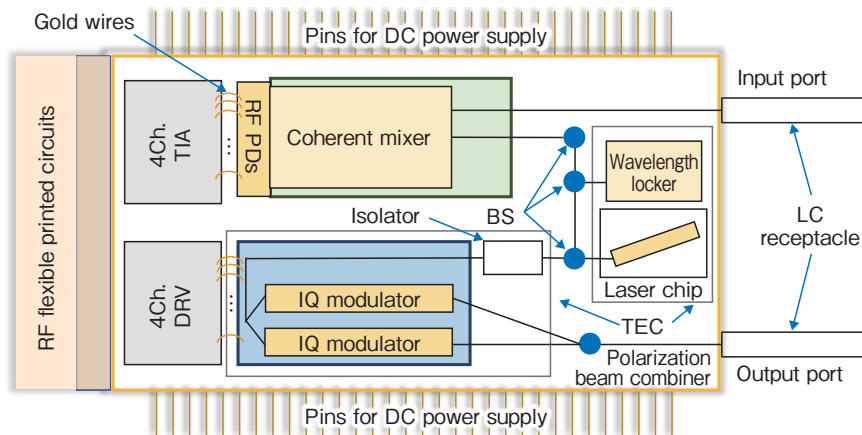


Figure 1 Schematic illustration of the IC-TROSA Type-2.

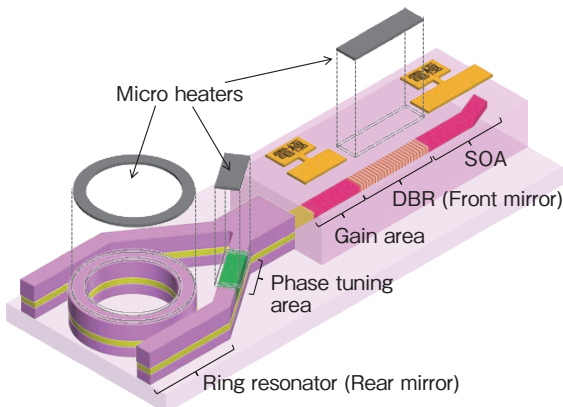


Figure 2 Schematic illustration of the wavelength-tunable laser chip.

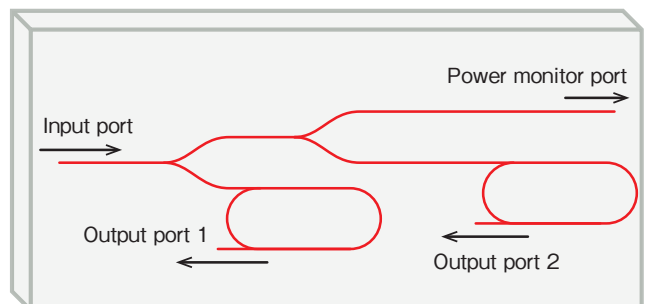


Figure 3 Schematic illustration of the PLC-based wavelength locker.

displacement of lens attachment. In addition, the modulator can extend an electrical bandwidth by adopting a capacitively loaded traveling wave electrode (CL-TWE). These designs contributed to achieving a small modulator chip size of 9.1 (L) × 3.3 (W) mm, a wide bandwidth of > 40 GHz, and a low driving voltage of 1.5 V[Ⓟ]. The modulator and the modulator driver are connected with gold wires of 20-μm diameter.

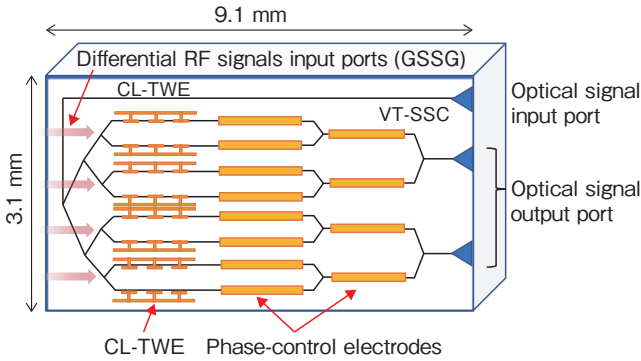


Figure 4 Schematic illustration of the InP-based modulator.

The receiver consists of a PLC-based coherent mixer, an InGaAs PIN-PD array and a 4-channel TIA. A schematic illustration for the PLC-based coherent mixer is shown in Figure 5. A facet in the right-hand side has a local oscillator (LO) input port, a signal input port and an output port for a monitor PD. A variable optical attenuator (VOA) and a polarization beam splitter (PBS) are placed in the signal light path. The coherent mixer interferes with the signal light and the LO light in a 90-degree optical hybrid to extract the phase information. After dividing the light into 8 ports from X-I to Y-Qn according to the phase, its output is coupled to the PD array on the backside. Figure 6 shows a schematic illustration of the InGaAs PIN-PD array mounted on a substrate. We employed a backside-illuminated 8-channel PD array which integrates a lens array on the backside to effectively enlarge the aperture size while maintaining a small active diameter. Figure 7 shows optical-to-electrical (O/E) responses. The

O/E response of the PD with various reverse bias voltages is shown in Figure 7(a). A 3-dB bandwidth of ≥ 49GHz can be obtained when the reverse bias voltage ≥ 1V is applied. To connect the electrodes of the PD and the TIA, a glass substrate with high-speed transmission lines was implemented. The transmission lines formed on the top surface are connected to the TIA with wire bonding. A common cathode electrode (C) is formed between two anode electrodes (A) in the differential channels. To mini-

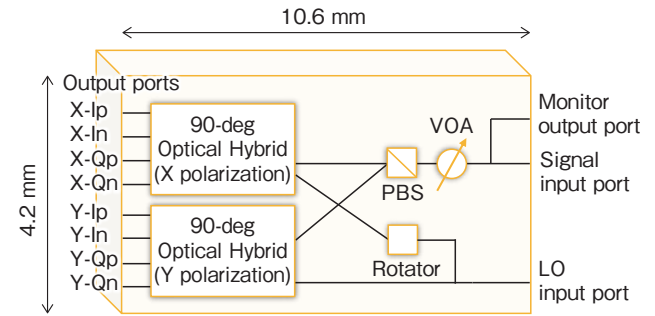


Figure 5 Schematic illustration of the PLC-based coherent mixer.

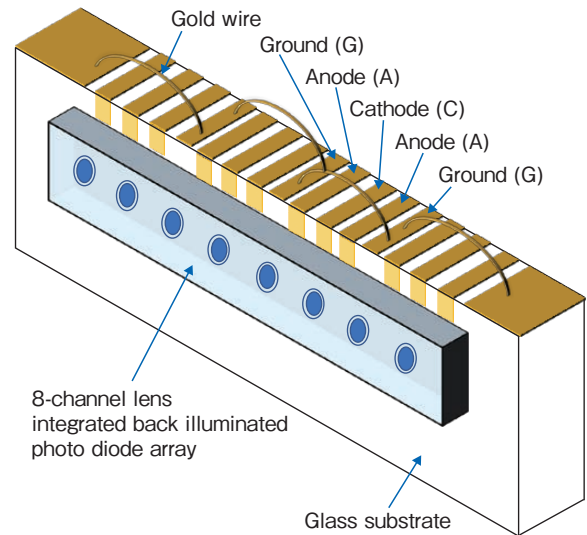


Figure 6 Schematic illustration of the PD sub-assembly.

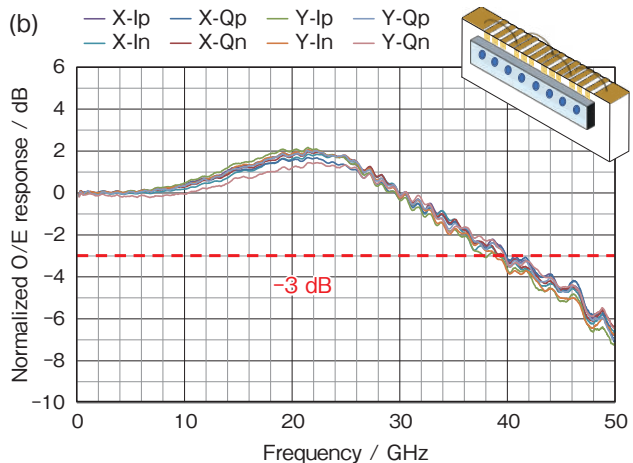
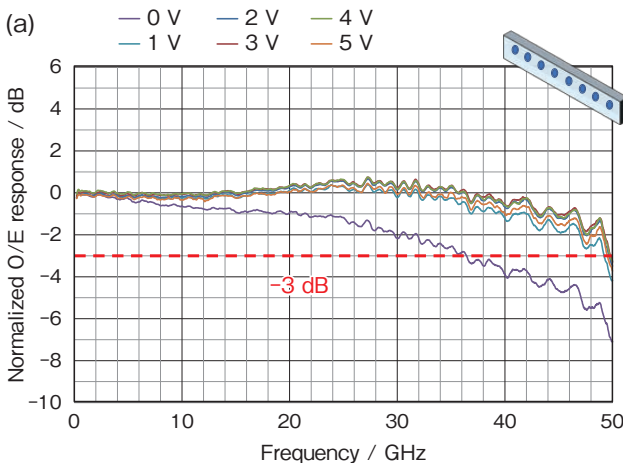


Figure 7 O/E responses (a) PD and (b) PD sub-assembly.

mize electrical crosstalk, ground electrodes (G) are formed between signal lines. As a result, the electrode arrangement becomes in the order G-A-C-A-G. The ground electrodes are connected with a gold wire to minimize the wiring length. The 8-channel PD array is mounted on this glass substrate with a flip-chip bonding process. The measured O/E response of the PD sub-assembly is shown in Figure 7(b). The reverse bias was set to 2 V. The O/E responses of all eight channels from X-lp to Y-Qn show similar characteristics, and a 3-dB bandwidth of around 40 GHz was obtained for all eight channels. As shown in Figure 8, this PD assembly is attached to the PLC-based coherent mixer with UV adhesive to minimize the receiver size.

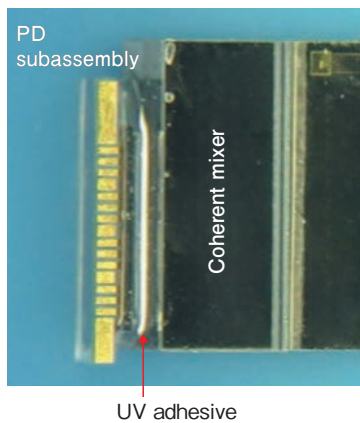


Figure 8 Photograph of the coherent mixer with the PD sub-assembly.

3. CHARACTERISTICS

Figure 9 shows a photograph of the prototype IC-TROSA Type-2 together with a dime. By minimizing the mechanical size of each component and adopting our hybrid-integration techniques, we successfully achieved a mechanical size of 26 (L) × 14 (W) × 4 (H) mm, which is smaller than the specified size of the OIF’s IC-TROSA Type-2 IA. In particular, the thickness is 2-mm thinner than the specified height. The smaller size can make wider clearances between piece parts and accordingly, it helps to integrate the TROSA into an optical transceiver together with control-ICs.

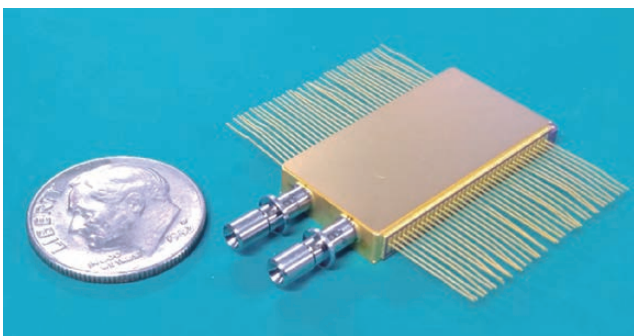


Figure 9 Photograph of the IC-TROSA Type-2.

Figure 10 shows a lasing spectrum of the built-in wavelength-tunable laser. We obtained a wavelength tuning range of 42 nm, which covers the entire C-band range. Figure 11 (a) shows misalignment tolerance curves of the focusing lens at the modulator-input port. The vertical axis is the normalized coupling loss, and the horizontal axis is the amount of lens misalignment. Measured horizontal coupling losses are plotted as red-square dots and measured vertical coupling losses are plotted as blue-diamond dots. Solid lines are the theoretical characteristics. The measured and the theoretical characteristics have a good agreement. Therefore, the lens is properly aligned as designed. Furthermore, the 1-dB loss width was $\geq 1 \mu\text{m}$ owing to integrated SSC, therefore the

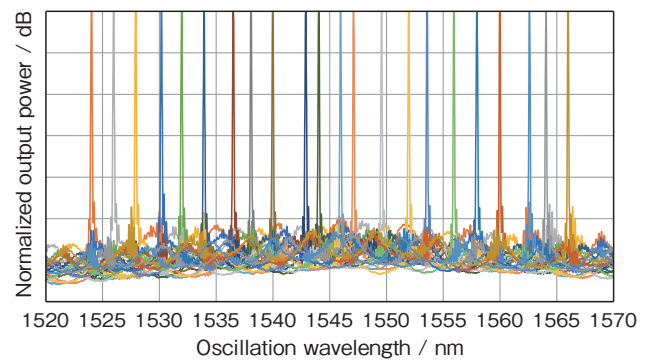


Figure 10 Lasing spectrum of the IC-TROSA Type-2.

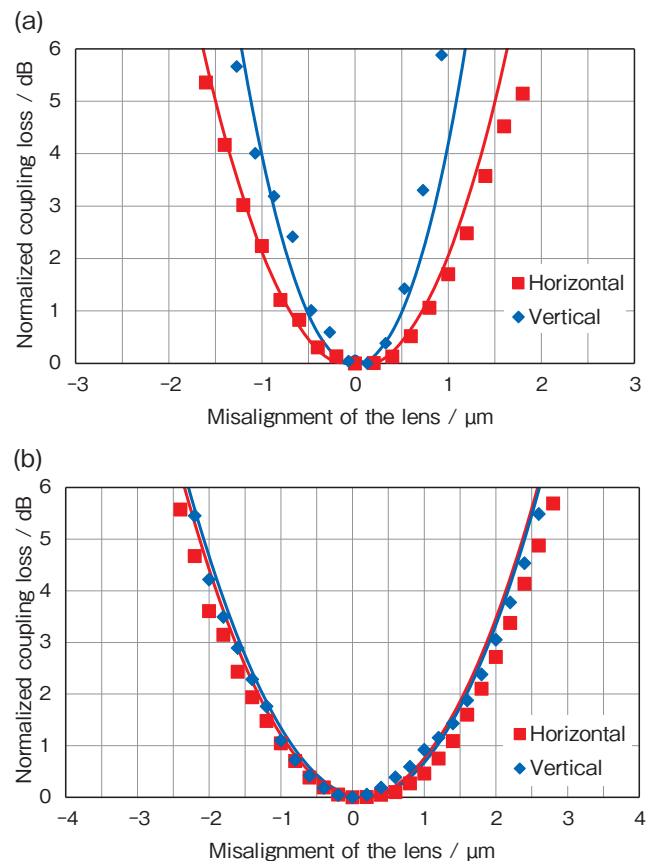


Figure 11 Coupling loss characteristics as a function of focus-lens displacement for (a) a modulator and (b) a coherent mixer.

lens position alignment range is sufficient. Similarly, Figure 11 (b) shows misalignment tolerance curves of the focusing lens at the coherent mixer signal input port. The results match the theoretical values in both horizontal and vertical directions. It indicates that the lens is assembled as designed.

Figure 12 shows insertion loss characteristics as a function of wavelength. Red dots plot the loss on the transmitter side. The insertion loss of the transmitter over the entire C-band is within 13.6 dB, including the branching loss to the receiver side (approximately 1.25 dB) and an isolator loss. When the laser chip output-power is controlled to be 17.5 dBm, the output power from the IC-TROSA is ≥ 3.9 dBm over the entire C-band. Similarly, the insertion loss of the receiver is plotted as blue dots. The loss is < 12.4 dB and almost constant regardless of the wavelength.

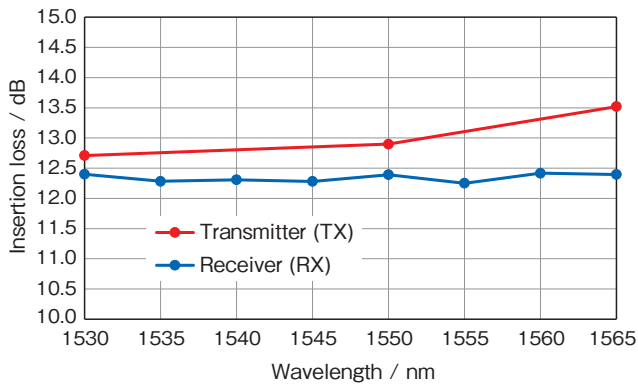


Figure 12 Insertion loss characteristics as a function of wavelength.

Then, we verified frequency response characteristics. An electrical-to-optical (E/O) response characteristic of the particular channel (X-Q) of the transmitter is shown in Figure 13 (a). We fed an electrical signal to the IC-TROSA using an RF probe to modulate the lightwave outputted from the tunable laser in a room temperature condition. The laser was operated at a constant temperature of

45°C. As shown in the figure, a 3-dB bandwidth of 45 GHz was obtained. Figure 13 (b) shows an O/E response characteristic of the receiver's particular channel (Y-Q). Same as on the transmitter side, an RF probe was used for the measurement. Thanks to a peaking functionality of the TIA, the measured 3-dB bandwidth was as high as 46 GHz and it was higher than that of the PD sub-assembly. These E/O and O/E bandwidths are sufficiently higher than our target value of 40 GHz, which is required for a 400-Gb/s (64-Gbaud) operation.

4. DEVELOPMENT TOWARD A HIGHER SPEED (≥ 800 GB/S) OPERATION

For future higher-speed optical links, we examined the employment of higher-speed devices for the next-generation IC-TROSA Type-2 while maintaining its hybrid-integration concept. We implemented a modulator that has a low loss and a wider bandwidth with an n-i-p-n heterostructure. CL-TWE structure is used for the RF electrode and termination resistors are integrated on the chip. The InP-based modulator exhibits higher E/O bandwidth of ≥ 67 GHz, and V_{π} is ≤ 2 V⁹. This modulator and a 4-channel DRV with a bandwidth of ≥ 90 GHz are combined as an ultra-high bandwidth coherent driver modulator. A measured E/O response characteristic is shown in Figure 14 (a)¹⁰. A 3-dB bandwidth of 75 GHz was obtained even including the loss of the evaluation board. Therefore, a wide bandwidth can be expected with the IC-TROSA as well. Similarly, we combined a receiver chip that integrates a coherent mixer and PDs, and a TIA whose bandwidth is above 70 GHz. Figure 14 (b) shows a measured O/E response characteristic of the receiver using an RF probe. Although the measured data is limited up to 50 GHz due to the limitation of the measurement equipment, the bandwidth is obviously over 50 GHz. A high-speed operation of ≥ 800 Gb/s can be expected.

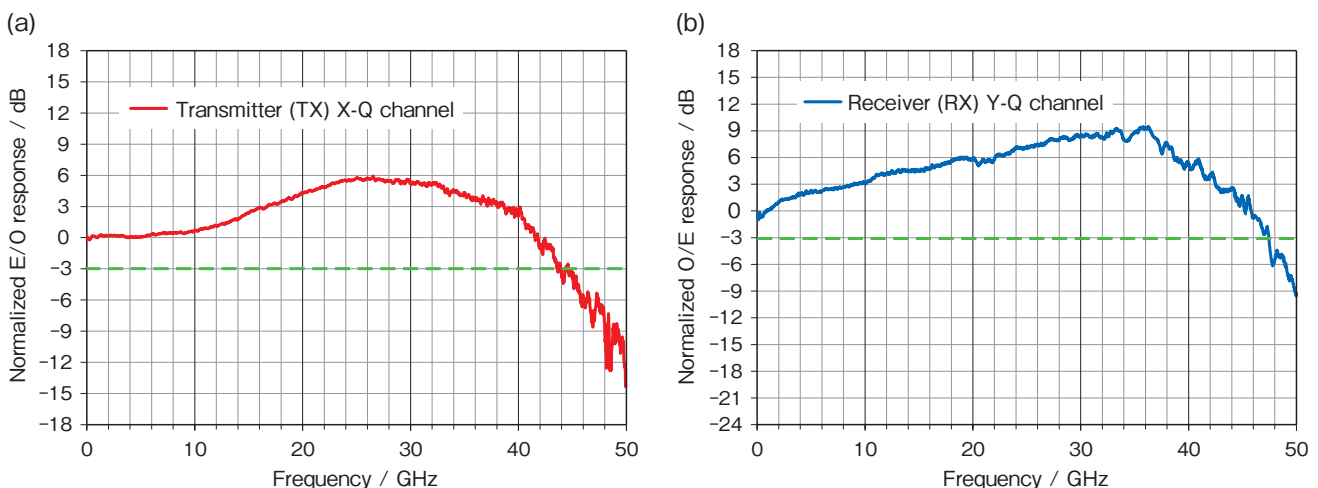


Figure 13 Frequency response characteristics (a) E/O response and (b) O/E response.

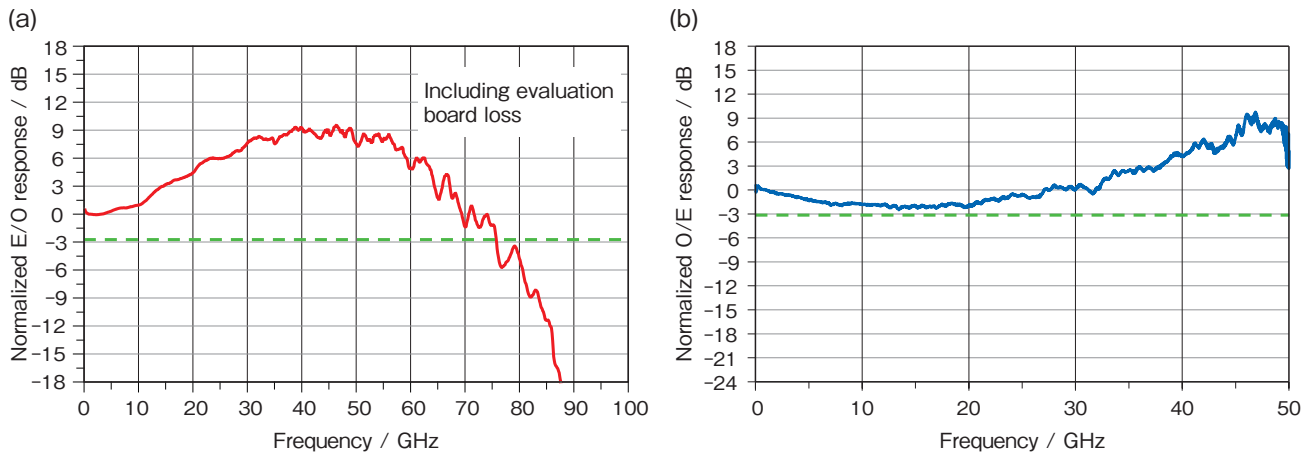


Figure 14 Frequency response characteristics for ≥ 800 Gb/s transmission (a) E/O response¹⁰⁾ and (b) O/E response.

5. CONCLUSION

We demonstrated an IC-TROSA Type-2 by hybrid integration of following components in a single package, those are a wavelength-tunable laser, an InP-based transmitter, and a PLC-based receiver. This IC-TROSA achieves the mechanical dimensions of 26 (L) \times 14 (W) \times 4 (H) mm, which is smaller than the specified size in the OIF IA for IC-TROSA Type-2. The built-in laser oscillation covers the entire C-band range. Low insertion losses of ≤ 13.6 dB on the transmitter side and ≤ 12.4 dB on the receiver side were achieved. We obtained E/O and O/E bandwidths of ≥ 40 GHz, which are sufficiently wide for ≥ 400 -Gb/s operations. We will develop the next-generation IC-TROSA Type-2 capable of ≥ 800 -Gb/s operation for supporting the advanced information society in the future.

ACKNOWLEDGMENT

We would like to thank NTT Device Innovation Center for their great cooperation in the achievement of these results, providing the high-frequency characteristics evaluation data of the 1-Tb/s-class ultra-high bandwidth coherent driver modulator, which is the result of their research and development.

REFERENCES

- 1) Implementation Agreement for 400ZR, IA # OIF-400ZR-01.0, March 10, 2020.
- 2) Quad Small Form Factor Pluggable Double Density MSA. [online] Available: <http://www.qsfdd.com>
- 3) OIF Launches 800G Coherent and Co-Packaging Framework IA Projects, Elects New Board Members/Positions, Officers and Working Group Chairs, (Referred on Dec. 8, 2020) <https://www.oiforum.com/oif-launches-800gcoherent-and-co-packaging-framework-ia-projects-elects-newboard-members-positions-officers-and-working-group-chairs/>
- 4) Implementation Agreement for Integrated Coherent Transmit-Receive Optical Sub Assembly, IA # OIF-IC-TROSA-01.0, August 20, 2019.
- 5) J. Hasegawa et al.: "32-Port 5.5-% Δ Silica-Based Connecting Device for Low-Loss Coupling between SMFs and Silicon Waveguides", in Proc. Optical Fiber Conf., 2018, Tu3A.4.
- 6) M. Nishita et al.: "The Development of a Nano-ITLA for Digital Coherent Datacenter Interconnects", Furukawa Electric Review, No. 52 (2021), 40-43.
- 7) M. C. Larson et al.: "InP vs Si Photonic Integrated Circuit Platforms for Coherent Data Center Interconnects", in Proc. European Conference on Optical Commun., 2018, 23-27.
- 8) Y. Ogiso et al.: "Over 67 GHz bandwidth and 1.5 V π InP based optical IQ modulator with n-i-p-n heterostructure", J. Lightw. Technol., vol. 35, no. 8, pp. 1450-1455, Apr. 2017.
- 9) J. Ozaki et al.: "Coherent Driver Modulator with Flexible Printed Circuit RF Interface for 128-Gbaud Operations", Photon. Technol. Lett. Vol. 34, issue 23, pp. 1289-1292, Dec. 2022.
- 10) J. Ozaki et al.: "Class-80 InP-based high-bandwidth coherent driver modulator with flexible printed circuit RF interface", in Proc. European Conference on Optical Commun., 2022, Mo4F.1.